JOURNAL OF MATERIALS SCIENCE **34** (1999) 2303–2312

# A preliminary investigation into preparation and characterisation of a Raney titanium catalyst

C. LIU, D. J. FRAY
*Department of Materials Science and Metallurgy, Pembroke Street, Cambridge CB2 3QZ, UK*
*E-mail: cll20@cus.cam.ac.uk, djf25@hermes.cam.ac.uk*

A preliminary investigation is carried out into the preparation and characterisation of a Raney-type titanium catalyst. Titanium-40 wt % aluminium powder is used as the precursor alloy and caustic leaching as the preparation method. Leaching in 25 wt % NaOH solutions at both 50 °C and 80 °C results in preferential removal of aluminium and formation of a highly porous layer containing almost complete titanium. The thickness and the surface roughness of the leached layer increases with leaching time and to a less degree with higher solution temperature. The combined morphological and kinetic measurements suggest that a diffusion barrier built up in the solution/metal interphas plays a key role in the leaching process. Electrochemical tests performed with the leached powder show a significantly reduced overpotential towards cathodic hydrogen evolution reaction, thus a potentially promising catalyst. Further work is needed to establish optimal leaching parameters to increase its electrochemical activity. 

## 1. Introduction

Large scale hydrogen production is considered as an alternative energy source, therefore research and development of techniques for bulk hydrogen generation, particularly from nonfossil primary energy sources, is both important and challenging [1, 2]. As one of the proven technologies in this field, water electrolysis is often the most cost-effective method comparing with gas reforming or coal gasification. Despite these advantages, the technology is restricted by the cost of electricity. The main focus of current research is to reduce its production costs through both fundamental research and optimisation of engineering factors involved.

Water electrolysis uses exclusively concentrated alkaline electrolytes (KOH or NaOH, 25–30 wt %), and the theoretical cell voltage for the decomposition of water can be calculated to be ca. 1.229 V at 25 °C and 1 atm. Cost analysis also indicates that the optimal current density lies between 0.5 and 1.0 A $cm^{-2}$ [1]. Since the current efficiency is close to 100% for the cathode, power consumption for operating a water electrolysis cell can be regarded as directly proportional to the cell voltage. Under a fixed cell configuration (anode/cathode distance, type of diaphragm, electrolyte concentration, etc.), the only parameter adjustable to decrease the cell voltage is the overpotentials governing the anodic or the cathodic electrochemical reactions. Hence the continued research to develop a better electrode/catalyst system is necessary.

There exists a few commercial catalysts for the purpose. A good example is Raney nickel catalyst and other nickel-based catalysts for both oxygen and hydrogen evolution reactions. In general, Raney catalyst is produced by preferential removal of an alloy constituent by a chemical reaction through caustic leaching which leaves porous and more noble metal network supported on the unaffected alloy substrate. The mechanistic and electrocatalytic aspects of the hydrogen and oxygen reactions have been extensively investigated and therefore forms useful guidelines in choosing suitable materials for potential catalyst development [3]. In addition, preparation methods also have a great influence on a catalyst's performance [4], because they determine issues such as specific surface area, electrical conductivity, long-term mechanical and chemical stability, as well as cost. It is generally known that the surface morphology and the specific surface area of the electrode greatly influence the electrode kinetics, therefore, electrodes with large specific surface area are being developed through electrodeposition, thermal spray, caustic leaching (Raney process), powder metallurgy and other methods which are capable of roughening the surface. Caustic leaching is one of the simplest methods.

Titanium has about half of the specific density of nickel, and is stable in concentrated alkaline solution and slightly more expensive. Titanium is also commonly used either as electrode substrates to support Raney Ni and other types of oxide catalysts or as added element to enhance catalytic properties of certain electrodes [5]. No literature exists, to the authors' knowledge, to show that porous titanium as an electrocatalyst is prepared through caustic leaching, although sintered porous titanium oxides has widely been used as electrocatalysts for chlorine production. It is therefore considered worthwhile to carry out a preliminary study to prepare a porous titanium surface through Raney process and subsequently characterise its electrochemical

activity. According to Miles [3], for the oxygen evolution reaction, Ni is the best catalyst while Ti is expected to be rather poor. We consequently concentrate our effort at this stage to develop a Raney titanium catalyst for the cathodic hydrogen evolution reaction.

## 2. Experimental

### 2.1. Precursor alloy

The composition of Ti-40 wt % Al alloy is (in wt %): Ti 59.01, Al 40.34, C 0.012, S 0.002, Si 0.21, V 0.02, Mn 0.04, Fe 0.24 and Cu 0.01. Under optical microscope, the microstructure of the alloy has three distinctive phases as shown in Fig. 1: the matrix plus two precipitation phases, one of which has many fine parallel dendrite-like plates. Scanning electron microscope (SEM) (Fig. 2) coupled with energy dispersive X-ray (EDX) analysis (Table I) reveal that the matrix phase is a TiAl solid solution, the circular precipitation phase has the composition of $Ti_3Al$ intermetallic, and the mixed phase has the composition close to an equal molar mixture of TiAl and $Ti_3Al$. Notice that the backscattered image (Fig. 2b) shows that the matrix phase (TiAl) seems more easily attacked by a NaOH based etchant, which is the phase corresponding to the highest aluminium content.

TABLE I EDX analysis of the Ti-40 wt %Al precursor alloy used. Only aluminium and titanium are analysed and therefore normalised to 100%. Other trace elements are not quantified

| Phases analysed | Aluminium | | Titanium | | Suggested formula | Trace elements |
|---|---|---|---|---|---|---|
| | at % | wt % | at % | wt % | | |
| Parent alloy | 55 | 40.34 | 45 | 59.01 | — | O, N, Ca |
| A | 49.64 | 35.70 | 50.36 | 64.30 | TiAl | Fe, Si, H |
| B | 43.28 | 30.07 | 56.72 | 69.93 | $TiAl + Ti_3Al$ | C |
| C | 31.08 | 20.25 | 68.92 | 79.75 | $Ti_3Al$ | |

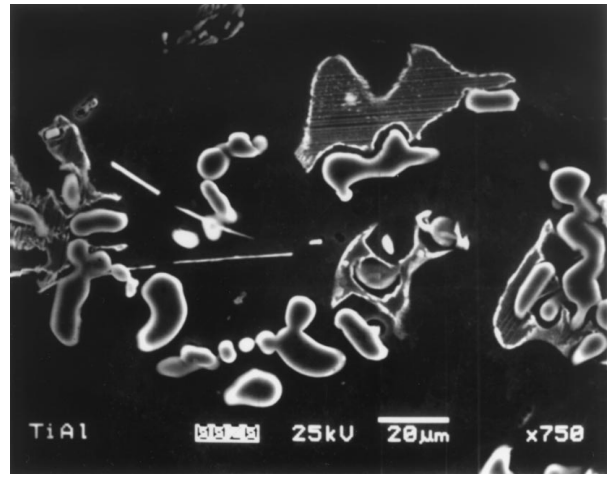


(a)

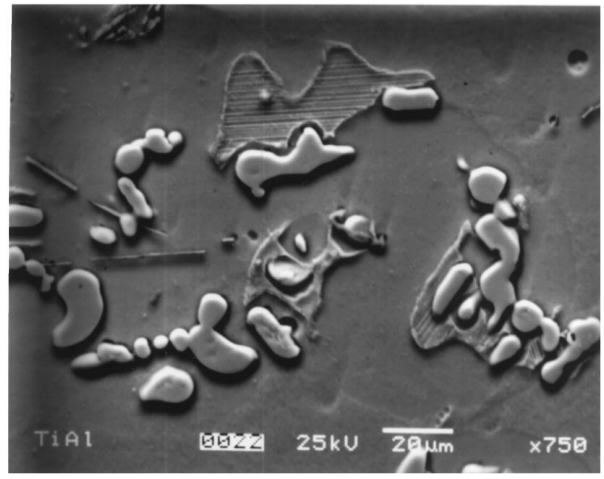


(b)

*Figure 2* The Ti-40 wt %Al precursor alloy in as-received state under SEM. In addition to the two types of precipitates found under optical microscope (Fig. 1), there seems to be an additional thin long precipitate. Backscattered image shows that the matrix is more easily etched than the precipitates: (a) Secondary electron image and (b) backscattered electron image.

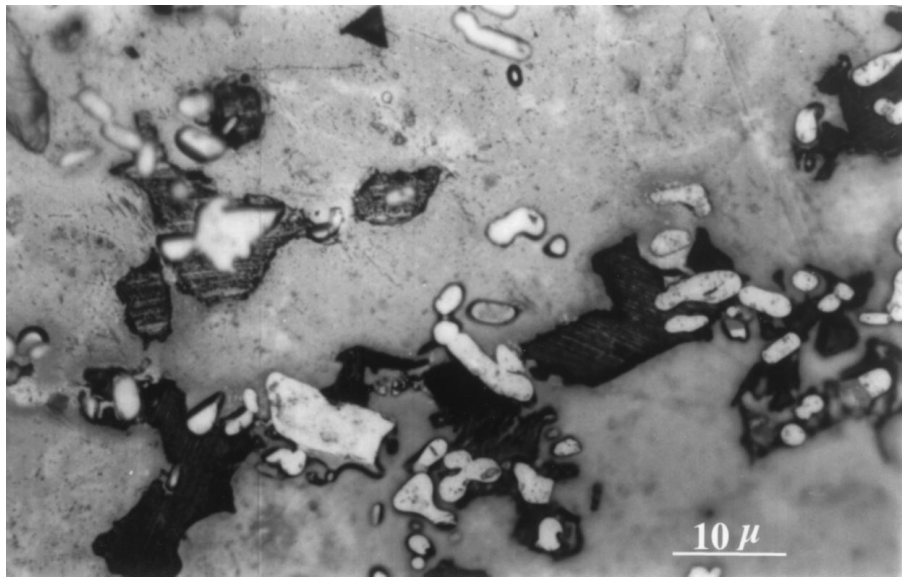


*Figure 1* Optical micrograph of the Ti-60 wt %Al precursor alloy in as-received condition. There are at least two types of precipitates on the matrix: one circular shaped with bright appearance and the other composed of fine mixtures of more than one needle-shaped phases.

The Ti-40 wt %Al precursor alloy is available in two kinds: one in large granular form with 10 to 30 mm in size, and the other in finely crushed powders with quoted particle size $\leq$500 $\mu$m. The former is suitable for preparing optical and SEM samples for microstructural analysis, whiles the latter is used for preparing the actual catalyst for its higher specific surface area. The two forms provide complementary information about the leaching kinetics and mechanism, as well as the activity of the catalyst prepared. Because the properties of the catalyst prepared is expected to depend on the particle size, the powder sample is further sieved into three groups with different particle sizes: Group I $\leq$ 45 $\mu$m, Group II from 45 to 125 $\mu$m, and Group III from 125 to 250 $\mu$m. The exact distribution of particle sizes within each group is unknown.

A 25 wt % (equivalent to ca. 6.3 M) sodium hydroxide solution is used for both leaching and subsequent electrolysis. This concentration corresponds to the highest electric conductivity at 80 °C [6]. Leaching is carried out in polypropylene bottles of 1 litre volume for each batch. These bottles are filled with 1000 ml 25 wt % NaOH solution and kept at the required temperature inside an incubation oven throughout the leaching process. After the solutions reach the pre-set temperature, ca. 20 g of the Ti-Al powder sample is added into each bottle. In parallel experiments, individually prepared large granular samples of the same alloy, each about 10 mm in size, are also leached under identical conditions. These large samples are designed to be individual specimen which can be taken out of the leaching process and examined at specified time intervals to give a snap-shot of the leaching processes. For this purpose, they have one side of their surface polished to 1200 grit finish, so that detailed microstructural information can be obtained. Furthermore, through SEM analysis on both the polished surfaces and the cross-sections perpendicular to them, leaching kinetics can be measured. Small amount of powder samples are also taken out at regular intervals for morphological examination by SEM. X-ray diffraction (XRD) spectra are also recorded with powder samples to reveal likely phase changes.

### 2.2. Electrochemical test

The electrochemical evaluation of the powders prepared is carried out in a three-electrode PTFE cell similar to that described by Chiba *et al.* for their tests with a Raney Ni catalyst [7]. The only difference is that our cell has no diaphragm because we are not concerned at this stage with the separation or purity of the gases. The cell has an immersion heater linked with a temperature controller for heating the solution to an elevated temperature; the accuracy of the temperature controller is within $\pm$2 °C. A mercury/mercuric oxide reference electrode is constructed with a half cell potential of ca. 0.927 V at 25 °C, and it is used as the reference electrode for all the electrochemical measurement. The leached powder to be tested is first weighed and then loaded directly onto a titanium substrate (commercial pure); no binder material is used. All the chemicals used are *Anala* grade and solutions are made up using distilled water.

## 3. Result

### 3.1. Physical characterisation

Morphological changes of the precursor alloy is most conveniently studied by using the large granular samples carrying polished facets leached at different time intervals. Typical results are grouped into three categories, *initial*, *intermediate* and *final*, according to their surface characteristics as a function of leaching time and are shown in Fig. 3. Because there is a possibility for aluminium leached out to form an adhering alumina gel to the surface in concentrated alkaline solutions, thus blocking the underlying features of the leached layer from being revealed, the samples are all subjected to 1 minute ultrasonic cleaning in warm distilled water prior to SEM observation. As will be shown by some of the photos in Fig. 3, the ultrasound wave is not only able to clean the surface, but also capable of "knocking out" some the leached surface layer at isolated local areas, particularly for those samples leached for longer duration.

Ignoring those features created by the "knocking out" effect, the main characteristics of Fig. 3 can be summarised as follows:

- *Initial leaching* ($\leq$12 h): it can be seen that the reaction between the alloy and NaOH is dependent on the alloy's phase structure at this stage. Each phase has different aluminium content and hence displays different chemical affinity towards the reaction. This is shown in Fig. 3A by the fact that the microstructure of the alloy is clearly visible, and in addition each phase is leached uniformly on macroscopical scale. The matrix phase however suffers extensive pitting;
- *Intermediate leaching* (from 12 to 48 h): substantial removing of aluminium occurs at this stage. It causes a leached layer with the appearance of "dry mud" to be visible both across the surface and also in depth towards metal substrate (Fig. 3B). Extensive cracks form between grains of the "dry mud", partially revealing the thickness at which the leaching has already taken place. There is very little sign of the original microstructure, indicating a change of leaching mechanism between the two stages. This new leaching mechanism dominates further leaching reactions and produces a rather uniform leached layer. Remains of the precipitation phases can still be seen occasionally, but they are unlikely to play a significant role in further leaching process as they appear to be semi-detached from rest of the surface;
- *Final leaching* ($\geq$96 h): Further leaching results in the width of the cracks to increase as well as more small cracks initiated within the original grains (Fig. 3C). This is believed to be caused by continued removal of aluminium within each grains, thus an increased volume shrinkage. However, the effect is small and no further significant decrease in

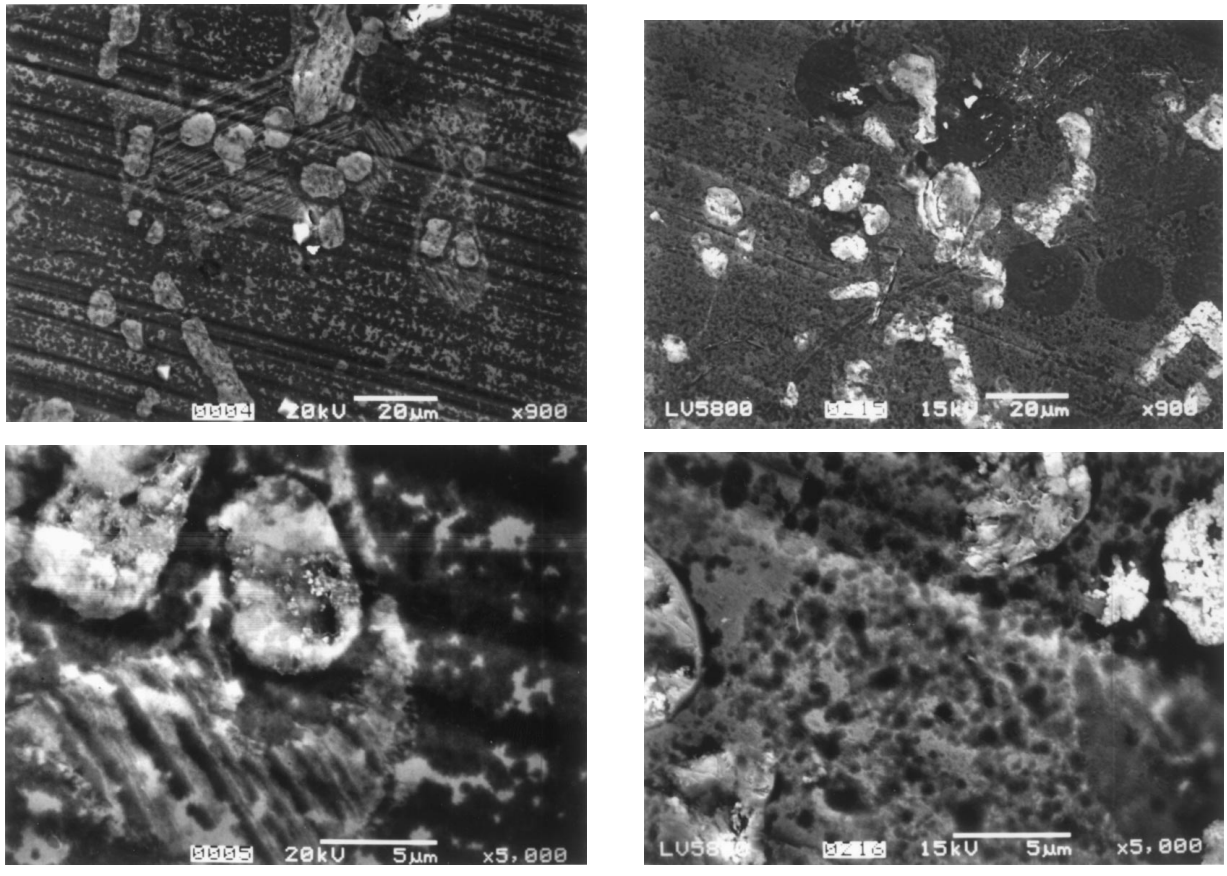


4 h 12 h

(A)

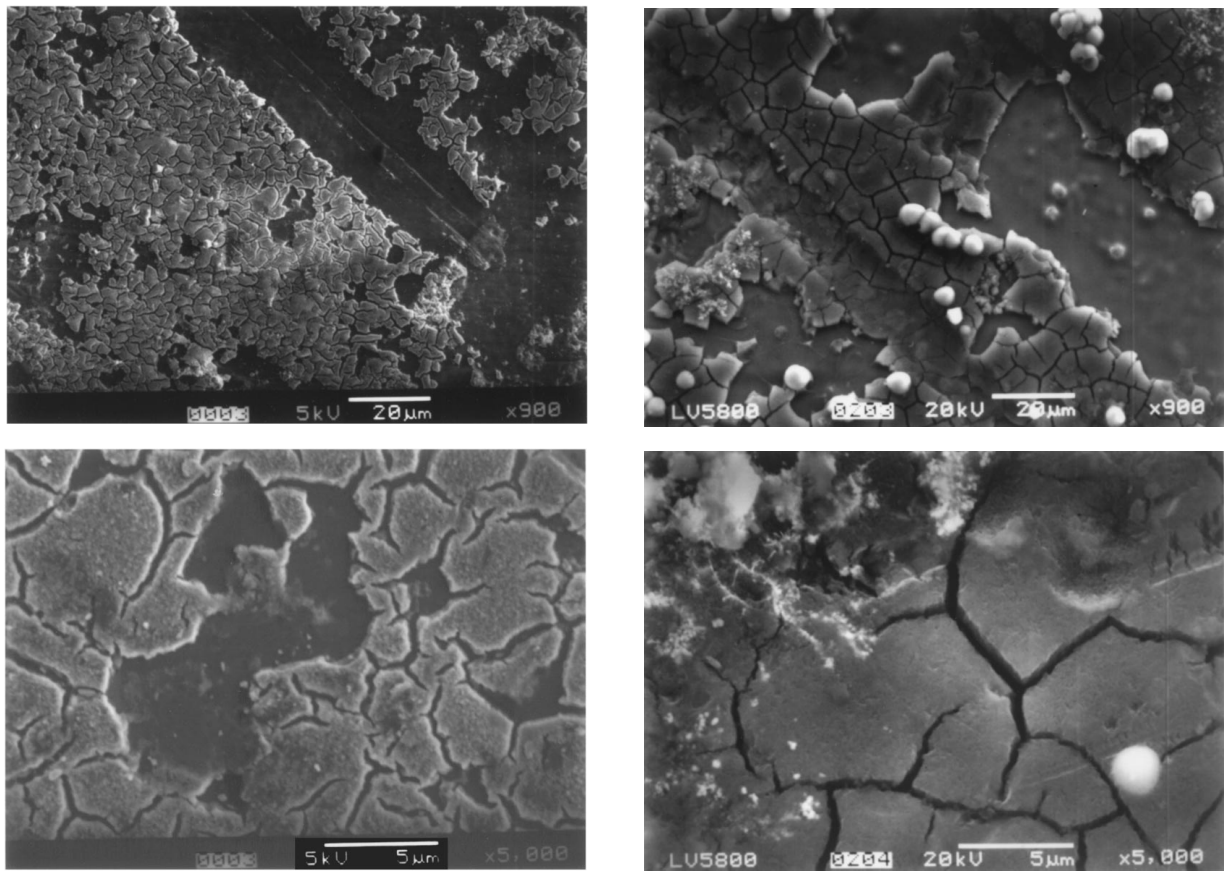


32 h 48 h

(B)

*Figure 3* Morphology change of the Ti-40 wt %Al precursor alloy leached in 25 wt % NaOH at 50 and 80 °C for different period of time (A, initial leaching; B, intermediate leaching; C, final leaching). Noticing that each sample is characterised under a low and a high magnifications. These samples are subjected to 1 minute ultrasonic cleaning in hot water. (*Continued* )

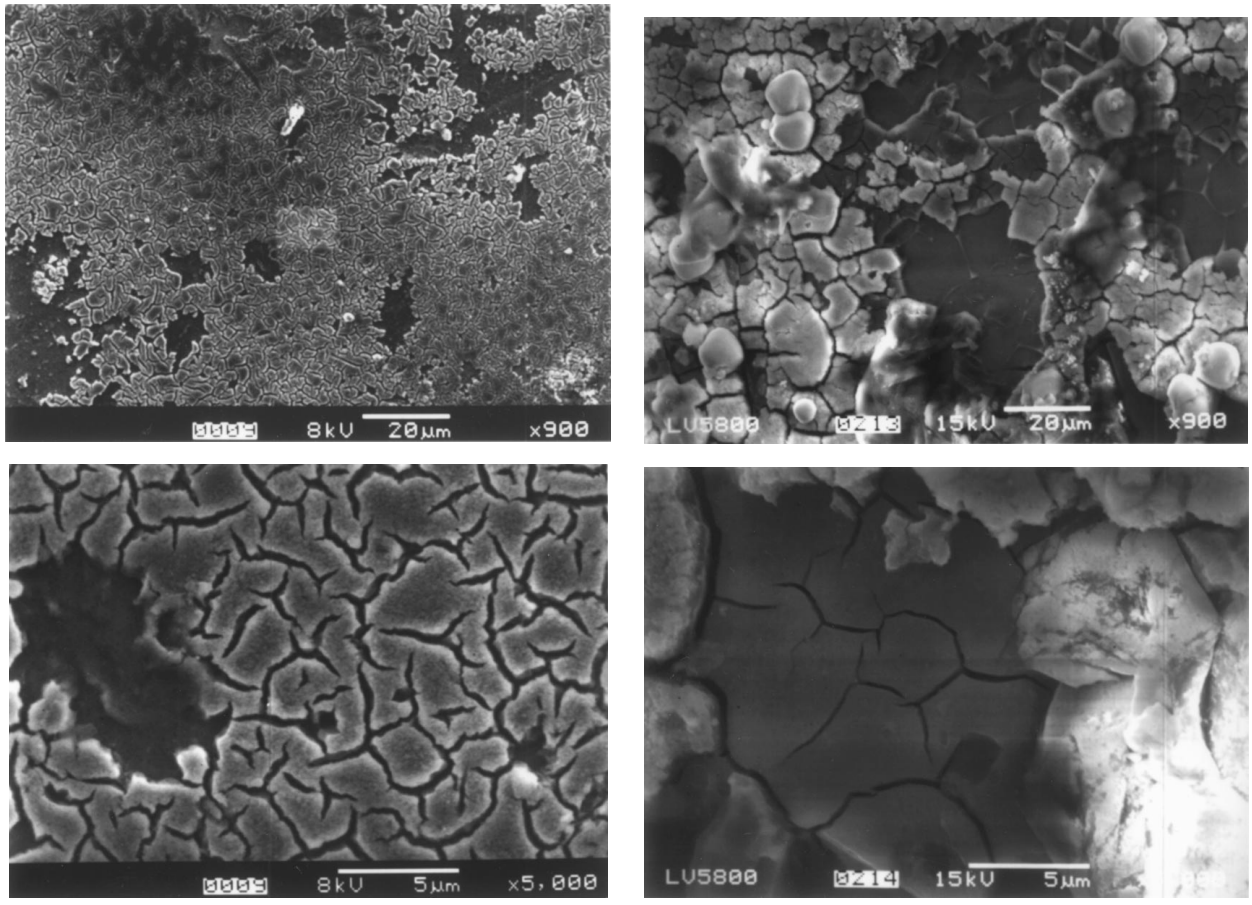


96 h 108 h

(C)

*Figure 3* (*Continued*).

the size or change in the shape of the grains is observed up to 108 h of leaching. The major progress of the reaction is the increase in the thickness of the leached layer.

Throughout the whole process, the difference between the appearance due to temperature increase is quite small. These observations suggest that the initial leaching proceeds via a chemical reaction controlled mechanism, which is later replaced by a mechanism possibly related to a diffusion-controlled mechanism. A diffusion barrier is likely to be built up because the removal rate of aluminium is high. This can be achieved either through the dissolved alumina layer adjacent to the alloy surface, or once a complete leached layer is formed (which is totally independent on the parent alloy's phase structure) through this leached layer, or through both layers. A more detailed account of the process is discussed later.

The above observations and comments of Fig. 3 are all made from bulk granular samples of ca. 10 mm in size which have been subjected to ultrasonic cleaning. One example of such a surface without pre-ultrasonic cleaning is shown in Fig. 4. The dry mud appearance is much more pronounced after 108 h of leaching, and the forms of the grains bear little relationship to their original phase microstructure. Except for only a few lost grains, the general features are almost identical to those shown in Fig. 3. Some of the cracks are seen to be filled with a gel-like material (possibly an aluminate).

The appearance of the powders (Group I with size $\leq 45\ \mu$m) after 108 h of leaching at 80 °C is given in Fig. 5. Fig. 5a shows random collection of particles after leaching. Due to their small size, the chance of finding cracks on individual particle is significantly smaller than a flat and larger sample as shown in Figs 3 and 4. Some of these particles are covered with nodule-shaped precipitates on their surface. These precipitates are thought to be the crystallised materials from the solution, most likely to be NaOH crystals as these particles are not ultrasonically cleaned and they are also more closely packed than the bulk granular samples. Nevertheless, a closer look still reveals clearly some large cracks which are similar to those observed with bulk granular samples (Figs 3 and 4). Furthermore, Fig. 5b also reveals large number of sub-micron pores which are previously unseen. These submicron pores are the major factor responsible for a high specific surface area, an potentially important parameter for any catalyst. The nodule-shaped crystals are also seen much clearer in Fig. 5b, their well-defined hexagonal shapes distinguish them from the occasional presence of the precipitation phases of the parent alloy (Fig. 2).

Fig. 6 shows the cross-sectional view of the leached Ti-40 wt % Al particles. The leached layer has a clear and reasonably well-defined boundary with the matrix alloy, and it appears slightly darker on the backscattered electron image (Fig. 6) due to the removal of aluminium atoms. Most of the cracks are extended straight towards the underlying matrix with an almost constant

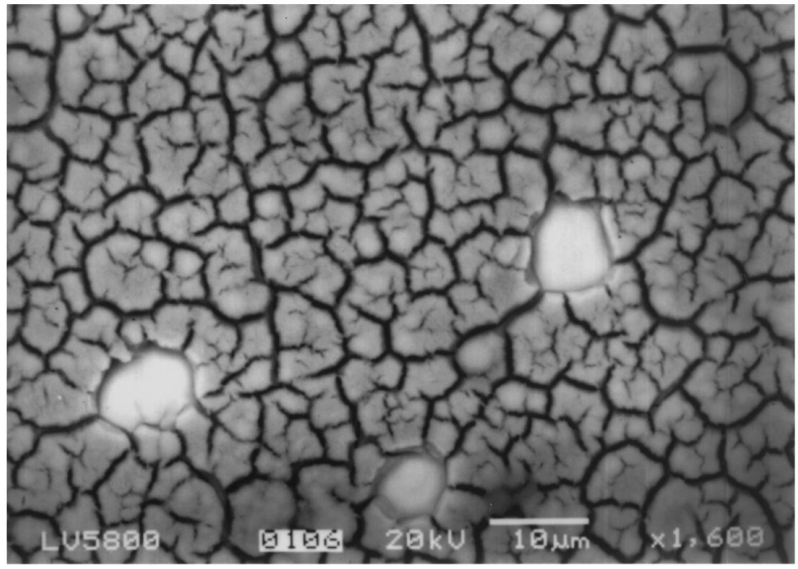


*Figure 4* The Ti-Al alloy surface leached in 25 wt % NaOH for 108 h at 80 °C: without ultrasonic cleaning.

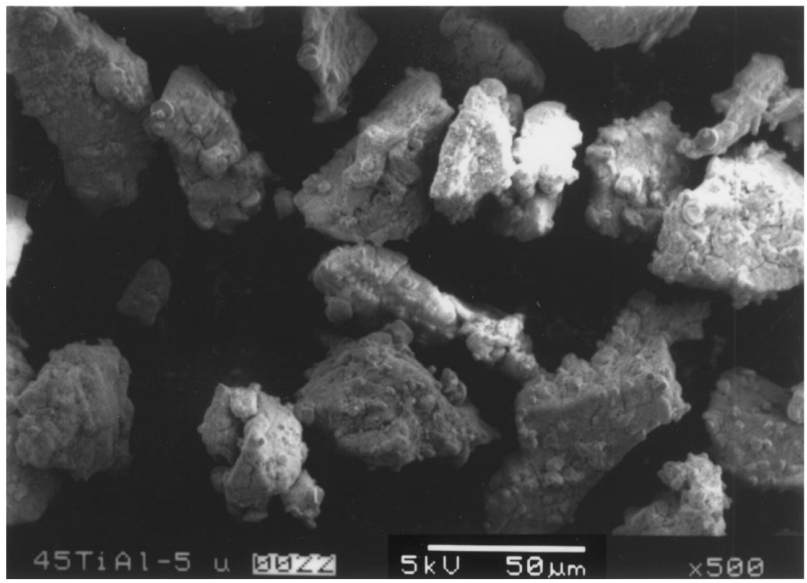


(a)

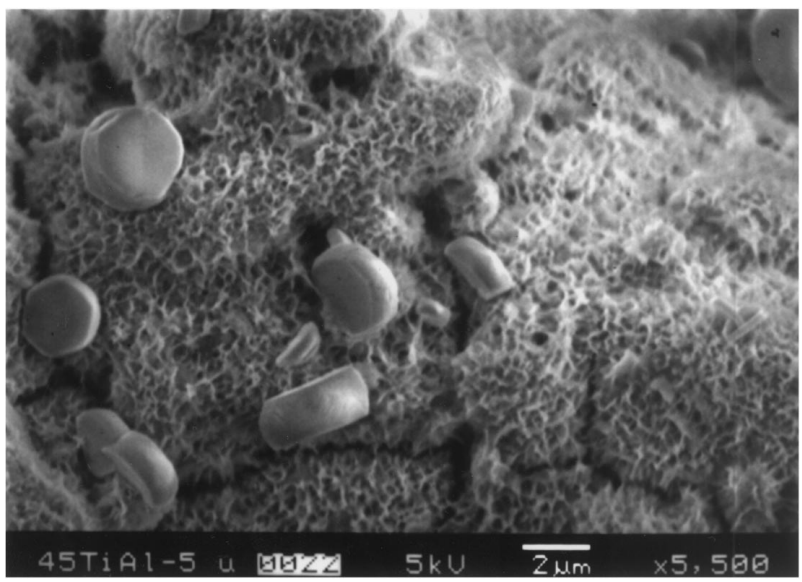


(b)

*Figure 5* The appearance of the Raney titanium catalyst prepared using the 45 $\mu$m precursor particles leached in 25 wt % NaOH at 80 °C for 108 h: (a) The overall appearance and (b) highly porous structure and some NaOH crystals attached on the surface.

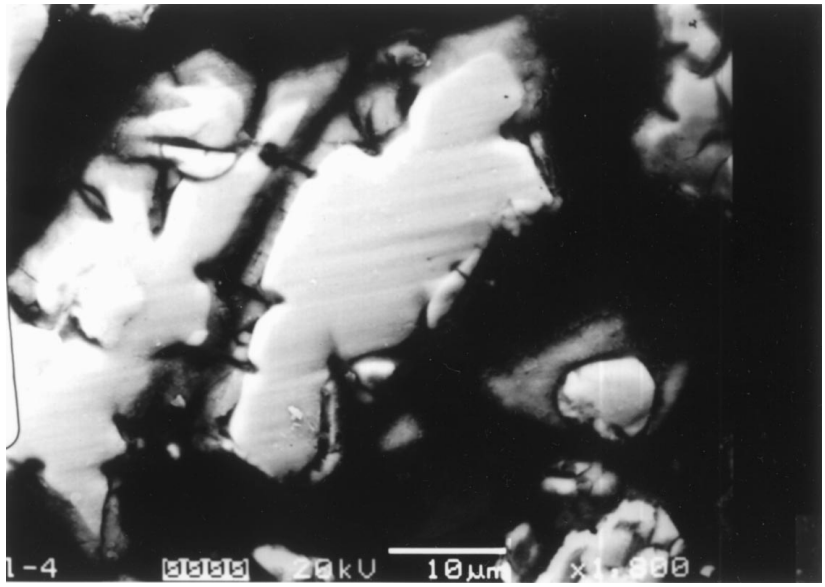


*Figure 6* The cross-section of the Raney titanium catalyst prepared using 45 $\mu$m precursor alloy in 25 wt % NaOH at 80 °C for 108 h.

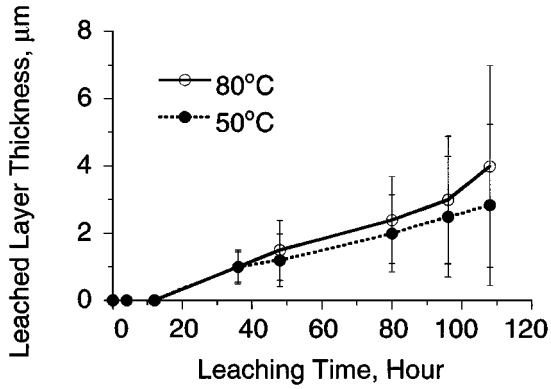


*Figure 7* The measured leached layer thickness as a function of leaching time and leaching temperature in 25 wt % NaOH solution. Measured using bulk granular samples under SEM. Error bar represents standard deviation of five repetitive readings.

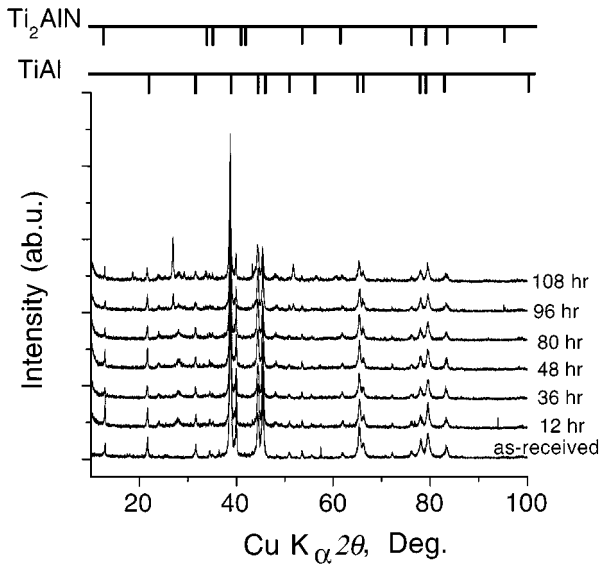


*Figure 8* XRD spectra prepared with the Group I ($\leq$45 $\mu$m) powder sample leached at different time intervals. In 25 wt % NaOH solution at 80 °C.

crack width, and the depth of the cracks also roughly coincide with the thickness of the leached layer. This seems to suggest that the removal of aluminium is rather uniform throughout the thickness of the leached layer and no significant gradient of aluminium exists within the leached layer, otherwise the cracks would become progressively narrow towards the matrix. EDS analysis on the leached layer (with cross-sections as shown in Fig. 6) gives hardly any aluminium on the leached layer, a direct evidence confirming the preferential removal of aluminium. Clearly the cracks are formed because of significant volume shrinkage and not due to other processes such as dehydration. It is less clear at this stage that whether or not the remaining titanium has to undergo a phase transformation to adapt to the significant volume shrinkage [8].

The clear distinction between the leached layer and the alloy matrix means that the thickness of the leaching layer can be measured with reasonable accuracy under SEM to provide quantitative information about leaching kinetics. The results are shown in Fig. 7 measured with the bulk granular samples, because it is more easy to prepare a cross section which is perpendicular to the original leaching surface. Fig. 7 suggests that the thickness of the leached layer increases almost linearly with leaching time, at least for the period of time investigated in this work. There is a small intercept on the time axis, roughly corresponding to the time taken for the microstructure dominated leaching reaction ceasing to be effective. The difference between the two temperatures is small.

Fig. 8 shows one example of XRD results prepared with the leached Ti-40 wt %Al powder samples (Group I $\leq$ 45 $\mu$m in size) in as-received state as well as leached at various stages. The XRD pattern shows that in addition to the strong peaks corresponding to the matrix phase TiAl, one of the dendritic precipitates consisting of $Ti_3Al + TiAl$ (however, it is most closely identified as $Ti_2Al(N)$ (18-0070) by a commercial software used, but thought to be the metastable mixture of the two phases with a composition near $Ti_2Al$) is also clearly

resolved. The presence of $Ti_3Al$ is almost completely masked by these two phases. Some broadened, low intensity peaks are also apparent, particularly at the low angle region, and they are likely to be structures relating to those of pseudo-beohmite or titanium oxide featuring random fine pores as shown in Fig. 5b. The XRD results obtained using the other two groups of powders, Group II ($45\,\mu m < size \leq 125\,\mu m$) and Group III ($125\,\mu m < size \leq 250\,\mu m$), have essentially the same characteristics, and therefore not shown here. The main conclusion of Fig. 8 is that the leached layer on the surface is still too thin to make a substantial contribution to the XRD spectra, for example, there is no indication of the presence of titanium. This may be explained by the fact that the penetration depth of the X-ray ($CuK_\alpha$) is likely to be deeper than ca. 10 $\mu$m, and the maximum depth measured in this work is less than 10 $\mu$m after 108 hours of leaching at 80 °C (Fig. 7). In addition, the surface layer is likely to be composed of various amorphous phases and its high number of cracks also favours the exposure of the matrix alloy. One of the practical implications is that XRD is not a sensitive method in monitoring the degree of the leaching reaction, at least within the initial stage.

## 3.2. Electrochemical characterisation

Electrochemical tests on the leached Ti-Al powders prepared in this work as a cathode for water electrolysis is performed in 25 wt % NaOH solution at different temperatures. In order to compare its performance, one commercial Raney Ni catalyst (a 50 wt % slurry in water from Sigma-Aldrich Co. Ltd.) is also tested under the same experimental condition. In both cases, the catalyst powders are simply packed on separate substrates (commercial pure Ni plate for Raney Ni catalyst and Ti plate for the leached Ti-Al powder, respectively) for ca. 1–1.5 mm in thickness, and no binder material is used to physically hold the catalyst layer on the substrate. Two consequences arise from this practice: one is that the catalyst loading in terms of weight per unit substrate area is not equal because the specific density of the two powders are different, and secondly the specific surface area of the leached Ti-Al powders is unknown, therefore, the comparison can only be treated as qualitative at most. The loosely packed powder also means that the application of large current densities or high potentials are restricted, as they tend to introduce vigorous evolution of hydrogen bubbles which can destroy the physical integrity of the catalyst layer. The highest current density used is 0.1 A $cm^{-2}$.

Typical results obtained from the leached Ti-Al powder are summarised in Figs 9 and 10. Fig. 9 shows that at 20 °C, the presence of the leached Ti-Al powder (Group I: size $\leq 45\,\mu m$) on top of the titanium substrate significantly raises the electrode potential, particularly at the lower current densities region. The increase in the electrode potential represents a decrease in cathodic overpotential, hence an activation of the electrode performance by the catalyst. However, the performance of the cathode loaded with the catalyst is somewhat fluctuating as shown in Fig. 9 by comparing its *E-i* characteristics with the smooth curve obtained with the titanium metal substrate. The level of fluctuation also increases with the increase of the applied current densities, and eventually the electrode with the catalyst exhibits an almost identical performance with that of the titanium substrate. This phenomenon is mainly caused by the release of hydrogen bubbles which is able to push some catalyst particles away from the substrate and to expose the substrate at these local sites. The measured electrode performance will then be a mixture of the bare metal substrate and the catalyst-bearing electrode. In the most severe case as can be seen in Fig. 9 that the performance of the Ti catalyst at 80 °C is almost impossible to measure except for lower applied current densities, presumably due to an enhanced evolution of hydrogen. Nonetheless, there is a small increase in the electrode potential with the Ti catalyst at higher temperature, most clearly shown at the lower current density region in Fig. 9.

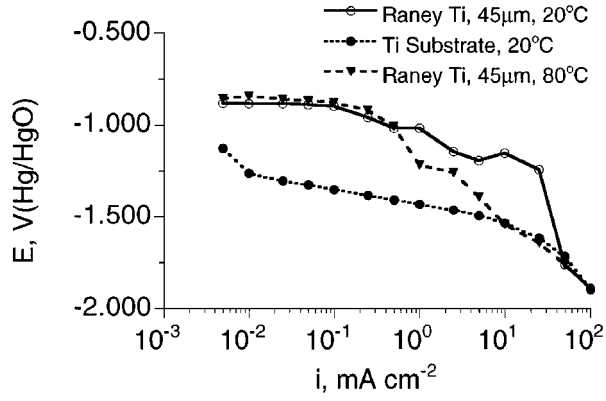


*Figure 9* The performance of the Group I ($\leq 45\,\mu m$) Raney Ti catalyst prepared in this work under different condition. In 25 wt % NaOH solution.

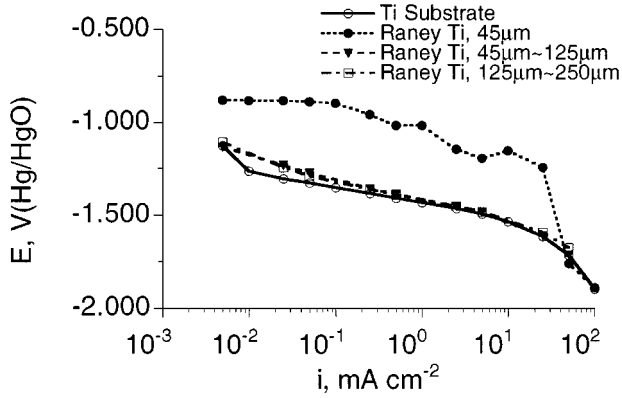


*Figure 10* The effect of particle size on the performance of the Raney Ti catalyst prepared in this work. In 25 wt % NaOH solution at 20 °C.

Fig. 10 illustrates the effects of particle size on the electrocatalytic activity of the prepared Ti catalyst. It indicates that the particle sizes have a dominant effect as expected: the two catalyst groups with larger particle sizes (Group II and III) show almost no catalytic activity at all the condition. Their *E-I* curves are also much more smoother than the electrode loaded with the 45 $\mu$m (Group I) powder under the same applied current densities. This suggests a reduced influence of the particle detachment caused by hydrogen bubbles due

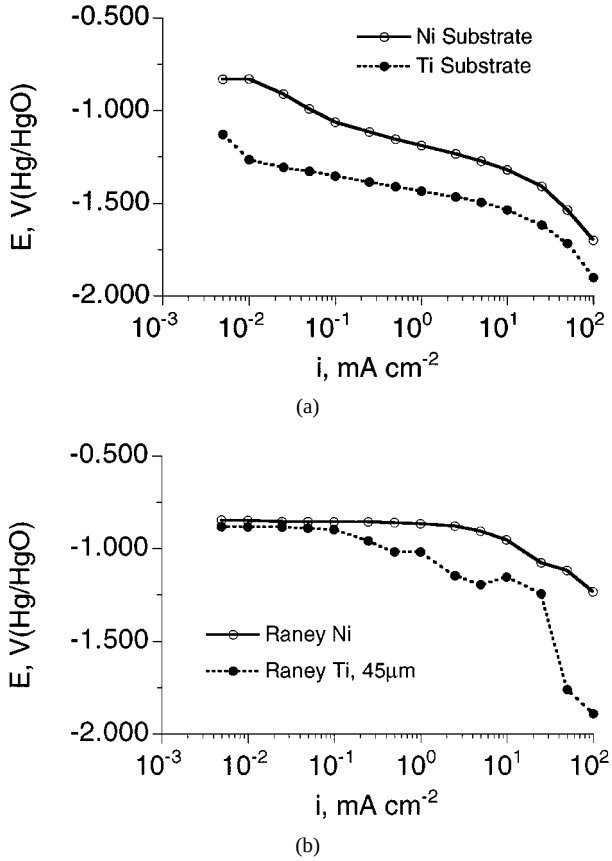


*Figure 11* Performance comparison of the two types of substrates and two types of Raney catalysts tested in this work. In 25 wt% NaOH solution at 20 °C: (a) The substrates and (b) the Raney catalysts.

to the larger and heavier particles. The much reduced electrocatalytic activities may be attributed to the combined effects of the reduced loading of the catalysts (for the same catalyst thickness), a decrease of the specific surface area per unit weight of loading and larger gaps between the catalyst particles which lead the electrolyte directly down to the substrate. Therefore, the comparison drawn here is more intuitive rather than conclusive.

Finally, to highlight both the success and the shortcoming of the prepared Raney-type Ti catalyst, an attempt is made to compare its performance with that of a commercial Raney Ni catalyst under same experimental conditions. The results are shown in Fig. 11 including the results from the two metal substrates. As shown by Fig. 11a, the intrinsic potential difference between the two metals is large at low current densities and tends to decrease towards high current densities; at the highest current density of 100 mA $cm^{-2}$ (1 mA $cm^{-2} = 10$ A $m^{-2}$) measured, the difference remains to be about 0.1 V. This reflects the fundamental difference of the two metals undergoing water electrolysis, and clearly shows that titanium has substantial lower activation energy towards hydrogen evolution reaction. By introducing catalysts, Fig. 11b further shows that Raney Ni greatly reduces the absolute value of the electrode potential, this in turn would bring down the cell voltage (assuming for a fixed anode and other experimental conditions), hence the energy consumption of running a water electrolysis cell. This result is in good agreement with previous literature [9–11]. Fig. 11b also shows that, despite the enhancement by the Raney Ti catalysts prepared in this work, the difference between the two cathode systems (substrate plus catalyst) at higher current density region remains almost the same with respect to the substrates. At the lower current densities, the performance of the prepared Ti catalyst is very closer to that of the Raney Ni catalyst. Notice also in Fig. 11b that the fluctuation is much less pronounced in the case of the Raney Ni than that of the Raney Ti, this is thought to be due to the higher specific density of Raney Ni catalyst, hence less affected by the hydrogen evolution. Work remains to be carried out to verify whether or not the large potential difference at the higher current density region in Fig. 11b is exclusively caused by the hydrogen evolution, which requires a suitable binder materials to be found for both catalysts and would eventually determine the feasibility of a new Raney Ti catalyst.

## 4. Discussion

The initial stage of leaching (Fig. 3) is clearly a chemical reaction controlled process, as different phases possess different reactivity towards NaOH and the microstructure of the alloy emerges. From the intermediate stage onwards, there is little relationship between the original microstructure of the alloy with the final "dry mud" appearance. The existence of a clearly defined boundary (almost parallel to the original geometric surface) between a uniform leached layer and the alloy matrix indicates that the leaching then proceeds at an equal rate across all the alloy phases. This observation suggests that original surface chemical reaction is replaced by another rate-controlling, and most likely chance would be the diffusion-controlled leaching mechanism set within the solution phase; otherwise surface roughening would continue to etch the metal and reveal the microstructure. Therefore, the initially different leaching reactions at the various phases/solution interface serves the purpose to remove aluminium at a sufficient fast rate to build up an aluminate diffusion barrier. Once the barrier is completed, the continuted removal of aluminium at the initially faster chemical reaction sites will face a higher aluminium concentration gradient, thus its rate being slowed down. Eventually, an apparent constant leaching rate across all the surface is established. The diffusion-controlled rate mechanism alters the final appearance of the leached surface, but the driving force to make aluminium break their initial bonds with titanium remains chemical in nature. As this reaction front moves deeper into the alloy substrate, the activity of $OH^-$ ions is expected to decrease because of the extreme narrow channels created by the leaching reaction. Eventually a steady state will be reached, and prolonged leaching will produce little further increase in the thickness of the leached layer. This kind of leaching behaviour has also been found in other alloy systems [12, 13].

The fact that initial microstructure of the alloy plays a less important role in determining the final appearance (hence to a large extent, catalytic properties) of the catalyst prepared, does not mean the alloy

composition is not important in the final performance of the catalyst prepared. This is because the remaining aluminium content in the leached layer is not quantified in this work (although qualitatively speaking, it is much lower than the parent alloy), and initial alloy composition may change the extent of aluminium left in the leached layer and hence its electrochemical performance. This remains a speculation at this stage. Nonetheless, the removal of aluminium is quite substantial, reflected by the extensive crack formation and the easiness by which some of the "dry mud" grains break away from the substrate with and without ultrasonic stimulation.

Fig. 11a shows that the h.e.r. may in fact follow different mechanisms on the two metal substrates, as $\partial E/\partial \log i$ is about 120 mV per decade for the Ni substrate and 80 mV per decade for the Ti substrate, except for higher current density regions ($\geq$ ca. 20 mA $cm^{-2}$). At higher current density region, the two $E$ vs. $\log i$ curves are almost parallel and their gradients $\partial E/\partial \log i$ increase with further rise of current density. This is likely to be caused by an enhanced *IR*-drop effect due to increasing amount of hydrogen bubbles being released near the electrode surface; only this effect is larger enough to mask the initial differences between the two substrates. When the catalysts are loaded respectively on the two substrates (Fig. 11b), their catalytic effects are most clearly reflected within the lower and the intermediate current density regions. Yet again the substantial release of hydrogen bubbles plays a dominant role on the electrode performance at the higher current density regions (Fig. 9) depending on the relative sizes or the specific densities of the catalysts, as described in the previous section.

It is shown in this work that caustic leaching can be used to preferentially remove aluminium atoms from the Ti-40 wt %Al precursor alloy and leave a Ti-enriched, highly porous surface layer. Although there are more work needed to be carried out before a complete relationship between the electrocatalytic activity of the porous titanium layer and the parent alloy composition and the best leaching condition, the results obtained so far point out the possibility to significantly enhance the electrochemical activity of titanium cathode for the h.e.r. and may be important for other areas utilising porous or spongy titanium surface. Finally, the performance as well as the potential application of the Raney Ti catalyst has to be evaluated with respect to the established Raney catalysts such as Raney Ni. As a preliminary investigation, the pore volume and the pore diameter associated with the Raney Ti catalyst prepared is not measured, neither its specific surface area. These parameter will have to be carefully measured as a function of other experimental conditions to achieve optimal electrocatalytic effect. The long-term stability of the catalyst is also a subject of future research.

## 5. Conclusion

An attempt is made to prepare a Raney Ti catalyst based on caustic leaching. It is demonstrated that substantial enhancement in the electrode performance can be achieved through the process. The electrocatalytic activity of the catalyst thus prepared strongly depends on leaching conditions as well as on the particle size of the precursor alloy. However, it is also found that the bonding between the Raney Ti catalyst layer thus prepared with its substrate appears to be weak; the problem may be solved through a suitable binder material or a precursor alloy with lower aluminium concentration.


## Acknowledgement

The authors thank London & Scandinavian Metallurgical Co. Ltd. for providing the Ti-40 wt %Al precursor alloy used in the work and Mr A. Misson for technical assistance.


## References


1. H. WENDIT and G. I. IMARISIO, *J. Appl. Electrochem.* **18** (1988) 1.
2. B. V. TILAK, P. W. T. LU, J. E. COLMAN and S. SRINIVASAN, in "Comprehensive Treaties of Electrochemistry," Vol. 2, edited by J. O'M. Bockris, et al. (Plenum Press, New York, 1981) p. 1.
3. M. H. MILES, *J. Electroanal. Chem.* **60** (1975) 89.
4. M. M. JAKSIC, *Electrochim. Acta* **29** (1984) 1539.
5. K. MUND, G. RICHTER and F.von STURM, *J. Electrochem. Soc.* **124** (1977) 1.
6. D. DOBOS, in "Electrochemical Data: A Handbook" (Elsevier, Amsterdam, 1975) p. 85.
7. T. CHIBA, M. OKIMOTO, H. NAGAI and Y. TAKATA, *Bull. Chem. Soc. Jpn* **56** (1983) 719.
8. J. SZOT, D. J. YOUNG, A. BOURDILLON and K. E. EASTERLING, *Phil. Mag. Lett.* **55** (1987) 114.
9. K. LOHRBERG and P. KOHL, *Electrochim. Acta* **29** (1984) 1557.
10. J. DIVISEK, H. SCHMITZ and B. STEFFEN, *ibid.* **39** (1994) 1723.
11. Th. BORUCINSKY, S. RAUSCH and H. WENDT, *J. Appl. Electrochem.* **27** (1997) 762.
12. J. B. FRIEDRICH, D. J. YOUNG and M. S. WAINWRIGHT, *J. Electrochem. Soc.* **128** (1981) 1840.
13. J. D. HARRISON and C. WAGNER, *Acta Metall.* **7** (1959) 722.



*Received 27 October*
*and accepted 18 November 1998*